AREA MEASUREMENT OF KNIFE EDGE AND CYLINDRICAL APERTURES USING ULTRA LOW FORCE CONTACT FIBER PROBE ON A CMM

B. Muralikrishnan, J. A. Stone, J. R. Stoup
National Institute of Standards and Technology
Gaithersburg MD 20899

ABSTRACT: Several radiometric and photometric measurements depend on high accuracy area measurement of precision apertures. Some apertures have sharp edges and are generally measured optically. At the Precision Engineering Division (PED) of the National Institute of Standards and Technology (NIST), we have developed a contact fiber probe for diameter and form measurement of micro-holes (holes of size 100 μm or larger). This probe exerts extremely small forces, under 5 μN, and can therefore be used on knife-edge apertures without causing edge damage. We have measured the diameter and roundness of three knife edge and one cylindrical aperture with this probe. The uncertainty in diameter ranges from 0.06 μm (k = 1) to 0.18 μm (k = 1). The uncertainty contributions from the probing system and machine positioning is together only 35 nm (k = 1). The largest contributors to the diameter uncertainty are the overall form (sampling uncertainty) and surface finish (mechanical filtering due to finite probe size) of the aperture.

1. INTRODUCTION

A major limitation to performing high accuracy radiometric and photometric measurements has been the accurate determination of aperture area. The diameter (and therefore the area) of apertures with land (cylindical apertures) are generally measured using a contact probe on a Coordinate Measuring Machine (CMM). These contact probes exert large forces, of the order of several milli-newtons, and are unsuitable for knife-edge apertures that have delicate edges. The area of knife-edge apertures is therefore generally measured by non-contact techniques.

Absolute non-contact techniques involve scanning the aperture on an *XY* translator while a sensor detects edge position. The translator, whose position is typically monitored interferometrically, establishes the metric and therefore such techniques are referred to as absolute area non contact techniques. The Optical Technology Division (OTD) at NIST has developed such an instrument [1-3] based on optical edge detection that comprises an interferometrically referenced *XY* stage, a microscope, and a charge coupled device (CCD) camera. The relative uncertainty in area ranges from 4.0×10^{-4} (k = 1) for 1 mm diameter aperture to 2.8×10^{-5} (k = 1) for 50 mm diameter aperture. Physikalisch Technische Bundesanstalt (PTB) in Germany has developed a non contact absolute system [4, 5] where a focused laser beam reflects off of the surface of the aperture. The reflectance is zero inside the aperture but is finite near the edge. The edge position is inferred from a known beam diameter. The relative uncertainties in area ranges from 2.1×10^{-5} (k = 1) for 20 mm diameter aperture to 8.4×10^{-5} (k = 1) for 5 mm diameter aperture.

The OTD at NIST has also developed a relative area measurement instrument [6-8] based on radiometric flux measurement. The area of the test aperture is determined by comparing the flux transmitted through this aperture against another aperture of known area. The relative uncertainty in area is 0.04 % for apertures of 2 mm to 25 mm diameter. PTB has developed a comparison technique applicable for apertures of small diameter, approximately 50 μm. The technique uses a trap detector to detect photocurrent of a reference aperture of known area. The photocurrent for the test aperture in combination with the photocurrent and area values of the reference aperture yields the area of the test aperture. They report relative standard uncertainty in area of 0.005 for apertures as small as 50 μm in diameter.

There are also other methods that attempt to directly measure the area [10-12]. A spatially uniform known irradiance is formed over the aperture by overlapping identical, parallel laser beams centered at constant spacing in an orthogonal lattice. The area is determined from the ratio of the throughput power and irradiance. The relative standard uncertainty in area is of the order of 1.6×10^{-4} for a 3 mm nominal diameter aperture.

In 1999, an international comparison of aperture measurement capability of different National Measurement Institutes (NMI) was conducted with NIST as the pilot lab [13]. It was found in this survey that the spread in measurement results was considerably larger than the uncertainties quoted by the labs. It was also determined that there was much larger variability in non-contact techniques than between contact techniques used by the different labs. However, the contact techniques were only applied to cylindrical apertures.

The ultra low force contact technique described in this paper offers a unique approach to the challenging problem of knife-edge aperture area measurement. Because the method can be used for the measurement of cylindrical apertures and other dimensional artifacts such as spheres, gage blocks *etc*, the results obtained from this technique can be easily compared against other known measurements.

We have measured the diameter and roundness of three knife edge and one cylindrical aperture that were previously part of that inter-comparison. In subsequent sections, we discuss the results from our measurements, sources of error, and compare our results and uncertainties with those listed in the inter-comparison.

2. THE NIST FIBER PROBE

Our technique, developed at the PED at NIST, incorporates a slender glass fiber as the probing element that undergoes cantilever deflection upon contact with the surface. We infer the position of the surface by monitoring the position of the fiber stem before and after deflection using two orthogonally placed microscopes. Figure 1 shows a schematic of the probe. The fiber is approximately 22 mm long. We have performed experiments with stem diameter as small as 50 μm. The diameter of the ball on the end is slightly larger than that of the stem. The microscopes image a point on the stem about 8 mm from the free end, allowing a working depth of that distance. The deflections of the stem as

determined from the camera images are in units of pixels; this is converted to units of micrometers using a previously determined calibration factor.

The probing system operates in two configurations, as a three-dimensional (3D) CMM probe [14, 15] and as a one-dimensional (1D) roundness probe [16]. In the CMM mode of operation, the probe is mounted on the Moore M48 CMM [17] at NIST and determines 3D surface coordinates. We have reported uncertainty in 16 sampling point least-squares best fit circle diameter as 70 nm (k = 2) [14].

In the roundness mode, the part is mounted on a precision spindle and the probe detects radial deviations. In order to overcome surface adhesive forces, the fiber is excited into resonance acoustically using a piezo buzzer as the part is rotated to present the next sampling position to the probe. We estimate the uncertainty in radial out-of-roundness to be under 200 nm (k = 2) [16].

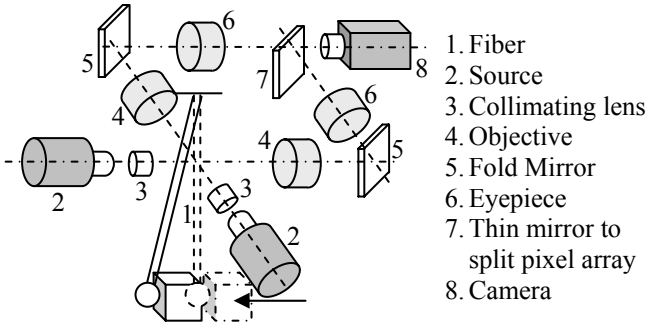

Figure 1 *Optical setup for fiber deflection measurement*

3. THE APERTURES

We measured the diameter and roundness of four apertures that were previously part of the inter-comparison [13]. In the intercomparison these apertures were designated 4, 13, 16, and 7. In addition, we also considered aperture 1 but do not present those results here. Aperture 1 on visual inspection under a microscope revealed considerable dirt near its edges. Our efforts at cleaning the edge resulted in an increase in diameter of 10 μm from values obtained prior to cleaning and we therefore suspect edge damage due to cleaning. Results and discussion of our measurements on apertures 4, 13, 16 and 7 follow in subsequent sections. The impact of dirt on uncertainty in diameter is discussed in section 5.2. Table 1 summarizes the properties of the four apertures considered in this study.

Table 1: Aperture information from Litorja *et al* [13]

ID	Diameter (mm)	Material	Edge Type	Fabrication
4	5	Cu	Sharp	Diamond turned
13	25	Al bronze	Sharp	Conventional
16	5	Al bronze	Sharp	Conventional
7	25	Al bronze	Cylinder	Diamond turned

4. MEASUREMENT APPROACH

Although area is the ultimate objective of our measurement, our immediate focus is the determination of diameter and its uncertainty, from which we compute the area and its uncertainty. We determine (and define) diameter by sampling 16 equally spaced points along the aperture's edge and fitting a least-squares best fit circle. Any reference to diameter in the text therefore implies the above definition being employed.

All diameter measurements are conducted with the probe in the CMM configuration. Preliminary measurements suggested that the knife-edge apertures have poor form. We therefore repeat the diameter measurement at three different locations along the edge, with each set of 16 point data indexed by 7.5° from the previous set. We report the average of the three 16-point diameters as the mean diameter.

The cylindrical aperture had substantially better form characteristics in comparison to the knife-edge aperture. The radial out-of-roundness of the cylindrical aperture was under 500 nm; we therefore only measured one set of 16 points.

Our measurement sequence involves several measurements of a calibration sphere to determine probe ball diameter and form, followed by check sphere and test artifact measurements. We used a variety of fiber geometries for diameter measurements. We refer to these as Fiber A, B, C and D. Their sizes are as follows:

- Fiber A: 125 μm diameter stem, 22 mm long with 200 μm diameter ball on the end. The probing plane is the equatorial plane of the ball
- Fiber B: 125 μm diameter stem, 22 mm long with the probing plane about 1 mm from the tip of the free end on the stem
- Fiber C: 50 μm diameter stem, 22 mm long, with the probing plane about 1 mm from the tip of the free end on the stem
- Fiber D: 50 μm diameter stem, 22 mm long, with 80 μm ball on end. The probing plane is the equatorial plane of the ball

As we discuss measurement results, we highlight the particular fiber that was used for that measurement. In section 5.2, we discuss the implications of using different fiber geometries.

In addition to diameter measurements, we also acquired higher density roundness data consisting of 192 sampling points with the probe in its roundness configuration. This high density data not only provides form information but is also used to estimate sampling uncertainty calculations as discussed in section 5.2.

5. KNIFE EDGE APERTURES

5.1 RESULTS

The diameters of the three knife-edge apertures measured using three different fibers are tabulated in Table 2. The radial form (as measured using Fiber B) of the three apertures with the probe in both the CMM and roundness mode are shown in Figures 2, 3 and 4.

Table 2: Diameter data (16 point sampling, least-squares best fit) for the different knife-edge apertures using three different fibers.

	Aperture 4			**Aperture 13**			**Aperture 16**		
Index Angle (°)	**Fiber A (μm)**	**Fiber B (μm)**	**Fiber C (μm)**	**Fiber A (μm)**	**Fiber B (μm)**	**Fiber C (μm)**	**Fiber A (μm)**	**Fiber B (μm)**	**Fiber C (μm)**
0.0	6585.16	6585.19	6585.21	25870.63	25870.71	25870.68	5206.03	5206.14	5206.12
7.5	6584.81	6584.76	6584.89	25870.82	25870.93	25870.96	5206.41	5206.41	5206.37
15.0	6584.98	6585.14	6585.16	25870.89	25870.97	25870.97	5206.50	5206.67	5206.62
MEAN	**6584.98**	**6585.03**	**6585.09**	**25870.78**	**25870.87**	**25870.87**	**5206.31**	**5206.41**	**5206.37**
SIGMA	**0.18**	**0.23**	**0.17**	**0.13**	**0.14**	**0.16**	**0.25**	**0.27**	**0.25**

The results tabulated in Table 1 and form plots in Figures 2, 3 and 4 indicate the influence of two factors that are expected to have significant impact on diameter uncertainty – sampling uncertainty due to part form and mechanical filtering due to finite probe size. We discuss these and other sources of uncertainty in this section.

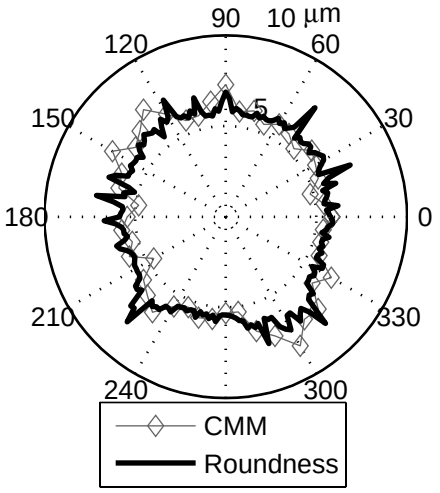

Figure 2 *Radial form of aperture 4*

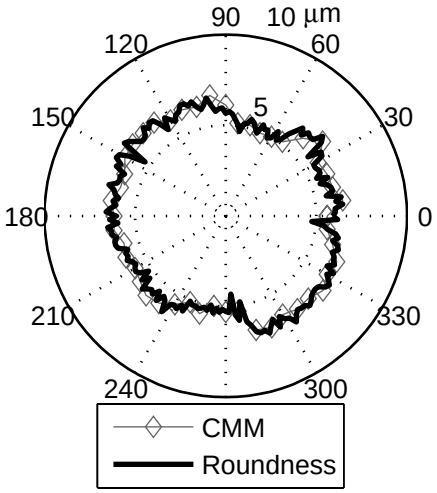

Figure 3 *Radial form of aperture 13*

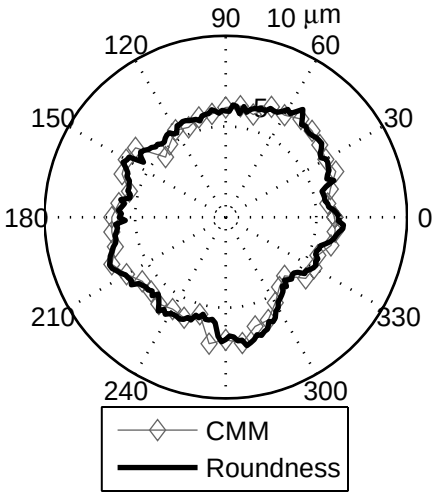

Figure 4 *Radial form of aperture 16*

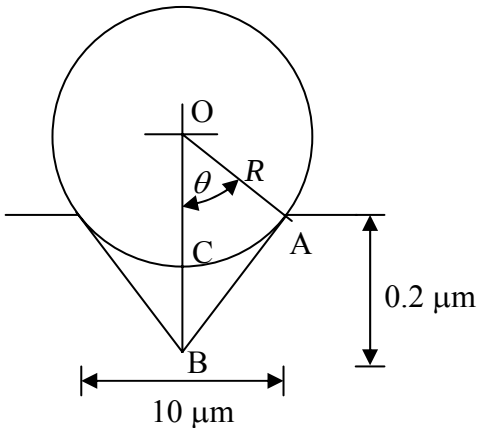

Figure 5 *A surface feature of 10* μm *width and 0.2* μm *depth measured with a probe ball of radius R. The dead space BC = R(1/cosθ-1). For R = 125* μm*, BC = 80* nm*. Assuming*

such features occur at diametrically opposite ends, the error in diameter is 160 nm*. For R = 100* μm*, this error is 100* nm *and for R = 50* μm*, it is 40* nm (Figure not to scale)

5.2 DISCUSSION

Mechanical Filtering

From the average diameter data in Table 1, the increases in diameter are 50 nm, 90 nm and 100 nm for apertures 4, 13 and 16 respectively when decreasing probe size from 200 μm (Fiber A) to 125 μm (Fiber B). This suggests the possibility of the occurrence of mechanical filtering. Further decrease in probe diameter does not indicate a strong trend; only aperture 4 shows any increase (60 nm) in diameter. The data suggests that aperture 4 has sharp features and that mechanical filtering may be a significant contributor to diameter uncertainty. The roundness trace for aperture 4 is indeed spiky, see Figure 2.

Theoretically, surface features of 10 μm width and 200 nm depth (slope of 1/25) can produce 60 nm changes in diameter when decreasing probe size from 200 μm to 125 μm and again from 125 μm to 50 μm. Assuming the surface has features at this scale, measurements performed using the 200 μm probe are smaller than the true value by 160 nm, measurements performed using the 125 μm probe are smaller by 100 nm and those performed using the 50 μm probe are smaller by 40 nm. Figure 5 illustrates this model.

We do not have sufficiently dense roundness traces with extremely thin fibers to carefully quantify the geometry, but we make the assumptions above for purposes of illustration.

While it appears that the measurements performed using the 50 μm probe should be closer to the true value, we have greater confidence in the measurements performed using the 125 μm probe because the thicker stem is less susceptible to environmental perturbations such as air currents.

Therefore, we will report the 125 μm stem data as the aperture's diameter. We will further assume that the true surface can lie anywhere between 0 to 100 nm from this value. Therefore the contribution due to mechanical filtering will be $100/\sqrt{3}$ = 58 nm. For aperture 4, we have some evidence that the true diameter may in fact be larger than the measured diameter and therefore the 58 nm term will be justified. But for apertures 13 and 16, the effect of mechanical filtering appears to be smaller. However, conservatively, we add the same 58 nm term for all three apertures.

It should be noted that the uncertainty due to mechanical filtering is a one-sided bias. The measured diameter value should be corrected for this bias to be in accordance with the Guide to the Expression of Uncertainty in Measurement [18]. However, the magnitude of the bias is unknown; the error of 100 nm is based on assumptions that may be incorrect. Therefore, we propose to retain our measured diameter value without any corrections but add the large uncertainty of 58 nm that will account for filtering effects that might plausibly be present.

Part Form

We measure 16 point diameter at three locations on the part. The spread in the diameter values (0.23 μm, 0.14 μm and 0.27 μm for apertures 4, 13 and 16 respectively) is therefore an indication of the uncertainty due to form. Because we report the average of the three diameters, the contribution due to form is $1/\sqrt{3}$ times the standard deviation in the diameters. Therefore, a possible estimate for form uncertainty is 0.13 μm, 0.08 μm and 0.16 μm for the three apertures respectively. We note however that because only three 16-point diameter measurements were taken, they may be insufficient to obtain a reliable estimate for uncertainty due to form.

However, for every aperture, we also have high density 192-point roundness measurements. While the radial deviation data is radius-suppressed, it still provides estimate for sampling uncertainty. This data can be partitioned into 12 sets of 16 equally spaced points. If we only consider the standard deviation in diameter from those three sets of 16 points that overlap the CMM data, the results are 0.23 μm, 0.11 μm and 0.18 μm for apertures 4, 13 and 16 respectively. These values are close to those obtained previously for apertures 4 and 13. For aperture 16, we note that two outlier points in the 7.5° orientation skew the diameter to the negative side. If these outlier points are ignored, the standard deviation reduces from 0.27 μm to 0.18 μm, which is in agreement with the roundness results. When we use the roundness data to estimate sampling uncertainty for aperture 16, the value is significantly less than the one standard deviation repeatability of the three CMM measurements. The additional uncertainty associated with aperture 16 is captured by a contribution for outliers, as discussed in the next section.

For purposes of determining reliable estimates for uncertainty due to form, we consider all 12 sets of 16 diameters. The standard deviation then turns out to be 0.20 μm, 0.17 μm and 0.10 μm for the three apertures. Because the reported diameter is the average of three 16-point diameter data, the form uncertainty is $1/\sqrt{3}$ times the standard deviation, which is 0.12 μm, 0.10 μm and 0.06 μm for three apertures.

Outliers (dirt)

The ultra-low force probing technique is extremely sensitive to dirt. While a traditional CMM probe exerting millinewton forces can possibly dislocate particles, our fiber probe is incapable of removing or crushing tiny particles on the part surface. Cleaning knife-edge apertures is also very challenging. Our attempts at cleaning aperture 1 only resulted in increasing the size of the aperture by 10 μm.

Interestingly, we have observed that our vibration assisted roundness measurement technique might actually serve as a non-destructive cleaning technique for these delicate edges. Figures 2 and 4 are evidence of this claim, where the roundness was measured after CMM measurements, and points that could conceivably be considered as dirt (see Figure 3, 150° and 330° points) in the CMM data are absent in the roundness data.

Because our efforts at cleaning aperture 1 were not successful, we measured the diameter of other apertures without cleaning the edges. Unfortunately, they were also measured prior to performing roundness measurements using the vibration assisted technique. The measured diameters, especially for apertures 4 and 16 are therefore smaller than the true diameter due to these outliers. We estimate an uncertainty of 42 nm for aperture 16 (2 out of 48 points appear to be offset by 1 μm each, see Figure 4) and 104 nm (5 particles each of size 1 μm, see Figure 2) for aperture 4.

Stem diameter variation

The diameter variation of the fiber stem (Fiber B) was measured to be 150 nm within a 1 mm portion of the stem. Local variations were about 20 nm within 5 μm along the stem. Stem diameter variation in combination with aperture warp or tilt will affect diameter measurements. The aperture warp/tilt is measured to be smaller than about 2 μm over the diameter and therefore the uncertainty is $20/\sqrt{3}$ = 12 nm.

Stem tilt

Any tilt in the stem will result in an erroneous calibration of its diameter. This error, given by $(Dc + Ds)*(\cos\theta - 1)$, where *Dc* and *Ds* are the diameters of the calibration ball and stem respectively, is 120 nm when stem tilt $\theta = 0.5°$, *Dc* = 3000 μm and *Ds* = 125 μm, and can therefore be substantial if the stem is not carefully aligned. We did carefully align the stem and the tilt was measured to be less than 0.05°. The error is therefore small, of the order of 1 nm.

Aperture tilt

If the aperture is tilted, the measured diameter will be the projection of the aperture on the horizontal plane, and therefore will be smaller than the true diameter. We have measured the tilt to be ±1 μm over the diameter of the aperture. The error due to tilt is larger for smaller apertures, but its magnitude is still extremely small, under 1 nm, for the smallest apertures (5.2 mm nominal diameter) we have measured.

Hertzian deformation

The contact between fiber B and the knife-edge aperture can be approximated as two orthogonal cylinders. The maximum compressive stress [19] is given by

$$\sigma_c = \frac{1.5P}{\pi c d}$$

where P is the applied force, $c = \alpha\sqrt[3]{PK_D C_E}$ and $d = \beta\sqrt[3]{PK_D C_E}$, α and β are coefficients that depend on the ratio of the edge diameter of the aperture and the fiber. C_E and K_D are given by

$$C_E = \frac{1-\nu_1^2}{E_1} + \frac{1-\nu_2^2}{E_2}$$

$$K_D = \frac{D_1 D_2}{D_1 + D_2}$$

where D_1 and D_2 are the edge diameters of the aperture and the fiber, E_1 and E_2 are the modulii of elasticity for the two materials, and ν_1 and ν_2 are the corresponding Poisson's ratios.

For fiber B of 125 μm diameter made of glass (E_1 = 70 GPa, ν_1 = 0.2) and a copper (E_2 = 120 GPa, ν_2 = 0.3) aperture with 1 μm edge radius, the contact force is of the order 4 μN, and the maximum compressive stress exceeds the yield strength for copper. (Note that the yield strength for glass fiber is much higher than for copper unless surface defects were present at the point of contact, leading to crack formation in the glass.) Consequently the copper aperture will plastically deform around the glass surface. As the glass sinks into the copper, the area of contact will increase, and therefore the contact stress will decrease, until the contact stress falls below the yield strength of the material. If we crudely model the plastically deformed contact area as the intersection of two crossed cylinders overlapping by some distance *z*, where we interpret *z* as the plastic deformation, then *z* is on the order of 1 nm when plastic deformation ceases. This small deformation is completely negligible for our application. Elastic deformation (as calculated via [19]) is also extremely small (under 2 nm), and consequently neither plastic nor elastic deformation poses any significant problem. For the 50 μm fiber, forces are much smaller and possible deformations are correspondingly decreased.

Probing uncertainty, machine positioning and other terms:

Probing uncertainty (imaging), machine positioning uncertainty, non-orthogonality of the probing axes, calibration sphere diameter and form uncertainty together contribute a standard uncertainty of 35 nm as reported previously [14].

5.3 COMBINED STANDARD UNCERTAINTY

The terms mentioned above are combined to yield the following uncertainties as shown in Table 3.

Table 3: Uncertainty budget for knife-edge aperture measurements

Term	Aperture 4	Aperture 13	Aperture 16
Probing uncertainty (μm)	0.035	0.035	0.035
Stem diameter non-uniformity (μm)	0.012	0.012	0.012
Stem tilt (μm)	0.001	0.001	0.001
Aperture tilt (μm)	0.001	0.001	0.001
Part form (μm)	0.116	0.100	0.058
Mechanical filtering (surface finish) (μm)	0.058	0.058	0.058
Dirt (μm)	0.104	0	0.042
Hertzian deformation (μm)	0.002	0.002	0.002
Combined standard uncertainty in diameter (μm)	**0.17**	**0.12**	**0.10**
Diameter (μm) (average of three 16-point diameters)	6585.03	25870.87	5206.41
Area (mm^2)	34.0569	525.6685	21.2896
Standard uncertainty in area (mm^2)	**0.0018**	**0.0049**	**0.0008**
Relative standard uncertainty in area	**5.2×10^{-5}**	**0.9×10^{-5}**	**3.8×10^{-5}**

It should be noted that we define the measurand, area, as computed using the least-squares circle diameter and not as the area enclosed inside the convex polygon formed by joining the sampling points by straight lines. The difference between these two methods is very small relative to the measurement uncertainty.

5.4 COMPARISON

The published area results (from [13]) for the three apertures from the participating NMIs in the inter-comparison are tabulated in Table 4. In the last row, we include the results of our measurements using the fiber probe along with the standard uncertainty. The results are also shown as a graph in Figure 6 (a), (b) and (c). Notice that the standard deviation of the diameter values reported is sometimes as high as ten times any stated uncertainty.

Table 4: Comparison of NIST fiber probe measurements with published results.

	Aperture 4		Aperture 13		Aperture 16	
	Area (mm^2)	Standard uncertainty (mm^2)	Area (mm^2)	Standard uncertainty (mm^2)	Area (mm^2)	Standard uncertainty (mm^2)
PTB	34.0262	0.0031	526.0117	0.1235	21.3321	0.0193
NPL	34.0189	0.0017	525.5218	0.0130	21.3082	0.0024
LNE-INM	34.0340	0.0054	525.6808	0.0490	21.2887	0.0043
MIKES	34.0240	0.0145			21.2690	0.0095
BIPM	34.0260	0.0016			21.2786	0.0011
VNIIOFI	33.9905	0.0022	525.4000	0.0110	21.2624	0.0009
OMH	34.0046	0.0179	525.5362	0.0620	21.2535	0.0109
NIST (OTD)	34.0291	0.0015	525.6332	0.0167	21.2789	0.0006
The NIST Fiber Probe:						
NIST (PED)	**34.0569**	**0.0018**	**525.6685**	**0.0049**	**21.2896**	**0.0008**

PTB (Physikalisch Technische Bundesanstalt): Germany, NPL (National Physical Laboratory): UK, LNE-INM (Laboratoire national de métrologie et d'essais: Institut National de Metrologie): France, MIKES (Mittatekniikan keskus Mätteknikentralen): Finland, VNIIOFI (All-Russian Research Institute for Optophysical Measurements): Russia, OMH (National Office of Measures): Hungary

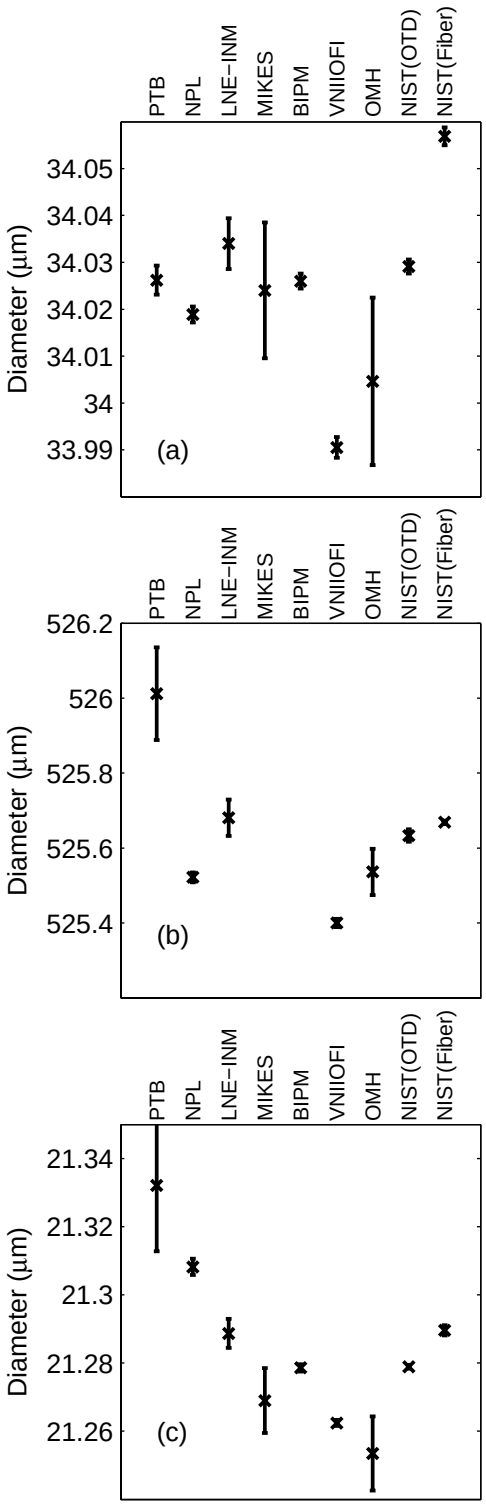

Figure 6 *Plot of nominal diameter values along with the standard uncertainty shown as an error bar for (a) aperture 4 (b) aperture 13 and (c) aperture 16*

We make the following observations:

1. Our uncertainty estimates are comparable to non-contact methods reported in the literature
2. The spread in the measurements reported by the NMIs in the inter-comparison is larger than their uncertainties and therefore, the uncertainties for the non-contact techniques are likely under-estimated
3. Our uncertainty claims on diameter (and area) can be validated by measurements on other artifacts such as cylindrical apertures. We discuss this in the next section.
4. The diameter values obtained using non-contact methods appear to be generally biased towards smaller values in comparison to our technique.
5. Our value for aperture 4 is larger than the mean of the different values reported by the NMIs by 0.0377 mm^2. While this may appear to be large, it should be pointed out that aperture 4 did demonstrate an increase in area of approximately 0.01 mm^2 during the duration of the inter-comparison between 1999 and 2003 (see Figure 5.3.10 in Litorja *et al* [13]), indicating that it is probably not a very stable artifact. At the present time we do not have an independent verification that the aperture area has increased since the 2003 measurements.

6. CYLINDRICAL APERTURE

6.1 RESULTS

The measurements were made with a ball-ended probe (a standard 50 μm stem, 80 μm ball probe, referred to as Fiber D in this paper). Only 16 sampling points were measured and only one probe geometry was used. However, because the aperture has a land area, we measured the diameter at different heights from the top surface. The results, averages of several runs, are tabulated in Table 5. Figure 7 shows the form plot. Note that the 0° position on the CMM data does not correlate with the 0° position on the roundness data for this aperture. The CMM data was acquired several months prior to collecting the roundness data and unfortunately no identification mark was placed on the part. We still plot the two sets of data in one graph to show the agreement in the overall scale, and to illustrate the generally smooth and excellent form which is in contrast to the poor form of knife-edge apertures.

Table 5: Cylindrical aperture measurement results

	Fiber Probe Diameter (μm) (16 point sampling)	Radial out-of-roundness (μm)	Area (mm^2)
38 μm below top surface	25361.92	0.56	505.1893
48 μm below top surface	25361.90	0.50	505.1885
58 μm below surface	25361.77	0.46	505.1833

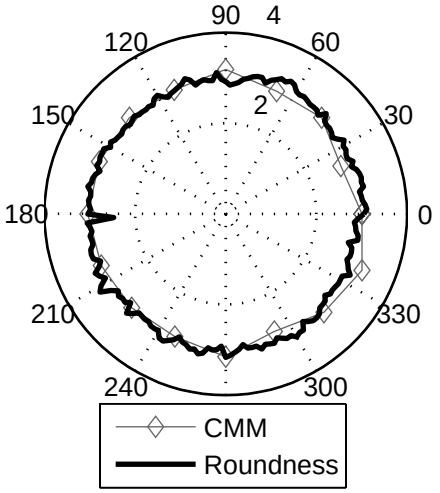

Figure 7 *Radial form of aperture 7*

6.2 DISCUSSION

The data in Table 5 indicates the presence of a negative taper in the aperture. This was confirmed by measurements made using the Movamatic probe on the Moore M48 CMM at NIST. The diameter value at 50 μm depth as recorded by the Movamatic probe was 25361.94 μm ± 0.11 μm. This value is only 40 nm larger than that determined using the fiber probe at 48 μm depth.

Mechanical filtering

Mechanical filtering is not expected to be a major factor as seen in the agreement between our values and values obtained using a more traditional probe on the M48 CMM at NIST.

Part form

Because the aperture has relatively small form (radial out-of-roundness of 500 nm) in comparison to the knife-edges, sampling uncertainty is expected to be smaller. While we did not measure 16 point diameter at 3 three different locations, such a measurement was performed using the Movamatic probe on the CMM. From that data, we determine the standard uncertainty in diameter due to part form to be 50 nm.

Other terms

Aperture tilt is as discussed in section 5.2. Other terms such as probing uncertainty, machine positioning uncertainty, *etc* are also as discussed in section 5.2. Uncertainties related to stem geometry are not relevant here because we use a ball-ended fiber.

Combined standard uncertainty

From the terms above, the combined standard uncertainty in diameter is 0.06 μm. The nominal diameter at 48 μm depth is 25361.90 μm and therefore the area is 505.1885 mm^2, and its standard uncertainty is 0.0024 mm^2. The relative uncertainty in area is therefore 0.5 x 10^{-5}.

6.3 COMPARISON

In Table 6, we list the published results of the measurements of aperture 7 in the inter-comparison. We also list the fiber probe values for comparison. Our results are in excellent agreement with other contact techniques, to within the stated uncertainties. Most non-contact techniques appear to be biased towards smaller area values, a trend we have observed with knife-edge apertures as well.

Table 6: Cylindrical aperture area comparison.

	NON CONTACT	
	Area (mm^2)	Standard uncertainty (mm^2)
PTB	505.1476	0.0509
NPL	505.1140	0.0130
LNE-INM	505.2272	0.0410
VNIIOFI	504.8890	0.0060
OMH	505.0377	0.0877
NRC	505.1750	0.0080
NIST	505.0708	0.0212
	CONTACT	
PTB	505.1755	0.0080
NPL	505.1827	0.0048
OMH	505.1665	0.0378
NIST (OTD)	505.1902	0.0026
The NIST Fiber Probe		
NIST (PED)	**505.1885**	**0.0024**

PTB: Germany, NPL: UK, LNE-INM: France, VNIIOFI: Russia, OMH: Hungary, NRC (National Research Council): Canada

7. CONCLUSIONS

We have developed an ultra-low force contact probe for the dimensional measurement of micro-scale features at the Precision Engineering Division at NIST. Using this probe, we have measured the diameter, area and roundness of three knife-edge and one cylindrical aperture that were previously part of an inter-comparison. We summarize the key results and observations here:

- The standard uncertainties in the area of the three knife-edge apertures we measured were 0.0018 mm^2, 0.0049 mm^2 and 0.0008 mm^2. These values correspond to relative standard uncertainties of 5.2 x 10^{-5}, 0.9 x 10^{-5} and 3.8 x 10^{-5}.
- The largest contributors to the uncertainty are not related to the probing system; rather the poor form and finish of the knife-edge apertures appear to be dominant elements in the error budget. A high quality knife-edge aperture will significantly reduce our uncertainties further.

- Cleaning knife-edge apertures is very challenging. The ultra-low force probing technique is very sensitive to dirt. It appears that our vibration assisted roundness measurement technique may be a non-destructive cleaning technique as well.
- Our method can be used for other dimensional artifacts, including cylindrical apertures. The standard uncertainty in area for the cylindrical aperture we measured was 0.0024 mm^2, which corresponds to a relative uncertainty of 0.5 x 10^{-5}. The cylindrical aperture diameter results show agreement of our technique with the more traditional Movamatic probe on the Moore M48 CMM to within 40 nm. This establishes the validity of our technique and the stated uncertainties.
- Our technique can be used for high quality apertures as small as 100 μm in diameter with relative standard uncertainty below 0.1 %. Smaller apertures can also be measured; we anticipate measurement of 50 μm diameter apertures in the near future using thin and short fibers.

ACKNOWLEDGEMENTS

We are grateful to the following colleagues for their help: Maritoni Litorja for providing the inter-comparison apertures and for valuable discussions, Eric Stanfield for roundness measurement of the calibration sphere, Tyler Estler, Ted Doiron and the two referees for carefully reviewing the manuscript and for their comments and suggestions particularly on the treating uncertainty contribution due to form, and Wolfgang Haller, Jeffrey Anderson and Fedor Timofeev for their help in manufacturing the fiber probes and advice in handing dirt and static issues during measurement.

REFERENCES

1. J B Fowler, R S Durvasula and A C Parr, High-accuracy aperture-area measurement facilities at the National Institute of Standards and Technology, Metrologia, 35 (4), 1998, 497-500
2. Fowler J B, Saunders R D and Parr A C, Summary of high-accuracy aperture-area measurement capabilities at the NIST, Metrologia, 37, 2000, 621–623
3. Fowler J and Litorja M, Geometric area measurements of circular apertures for radiometry at NIST, Metrologia, 40, 2003, S9–S12
4. Fischer J., Stock M., A non-contact measurement of radiometric apertures with an optical microtopography sensor, Measurement Science and Technology, 8, 1992, 693-698.
5. Hartmann J, Fischer J and Seidel J, A non-contact technique providing improved accuracy in area measurements of radiometric apertures, Metrologia, 37, 2000, 637–640
6. Fowler J., Dezsi G., High accuracy measurement of aperture area relative to a standard known aperture, Journal of Research of the National Institute of Standards and Technology, 100 (3), 1995, 277-283
7. Allan W Smith, Adriaan C Carter, Steven R Lorentz,Timothy M Jung and Raju V Datla, Radiometrically deducing aperture sizes, Metrologia, 40, 2003, S13–S16
8. James A Fedchak, Adriaan C Carter and Raju Datla, Measurement of small apertures, Metrologia, 43 (2), 2006, S41–S45

9. J Hartmann, Advanced comparator method for measuring ultra-small aperture areas, Measurement Science and Technology, 10, 2001, 1678-1682
10. Lassila A, Toivanen P and Ikonen E., An optical method for direct determination of the radiometric aperture area at high accuracy, Measurement Science and Technology 8 (9), 1997, 973-977
11. E Ikonen, P Toivanen and A Lassila, A new optical method for high-accuracy determination of aperture area, Metrologia, 35 (4), 1998, 369-372
12. M Stock and R Goebel, Influence of the beam shape on aperture, measurements with the laser beam scanning technique, Metrologia, 40 (1), 2003, S208-S211
13. Maritoni Litorja, Joel Fowler, Jürgen Hartmann, Nigel Fox, Michael Stock, Annick Razet, Boris Khlevnoy, Erkki Ikonen, M Machacs and Kostadin Doytchinov, Final report on the CCPR-S2 supplementary comparison of area measurements of apertures for radiometry, Metrologia, 44 (1A), Technical Supplement 2007
14. B. Muralikrishnan, Jack Stone and John Stoup, Fiber deflection probe for small hole metrology, Precision Engineering – Journal of the International Societies for Precision Engineering and Nanotechnology, 30/2, 2006, 154-164
15. Jack Stone, B. Muralikrishnan and John Stoup, A fiber probe for CMM measurements of small features, Proceedings of SPIE Vol. 5879 – Recent Developments in Traceable Dimensional Measurement III, San Diego, CA, 2005
16. B. Muralikrishnan, Jack Stone and John Stoup, Roundness measurements using the NIST fiber probe, Proceedings of the annual meeting of the ASPE 2007, Dallas, TX
17. Disclaimer: Data on commercial products are only provided for the sake of describing experimental results. NIST does not endorse or recommend any commercial products or imply that this equipment is the best for any particular application.
18. ANSI/NCSL Z540-2-1997, U.S. Guide to the Expression Of Uncertainty in Measurement
19. Warren C.Young, Roark's formulas for stress and strain, 6th Edition, McGraw-Hill Book Company, 1989